Solid State Communications 157 (2013) 54–57

Contents lists available at SciVerse ScienceDirect

Solid State Communications

journal homepage: www.elsevier.com/locate/ssc

Effects of superconducting film on the defect mode in dielectric photonic crystal heterostructure

Chung-An Hu [a], Jia-Wei Liu [b], Chien-Jang Wu [b,*], Tzong-Jer Yang [c], Su-Lin Yang [a]

[a] Department of Electrophysics, National Chiao Tung University, Hsinchu 300, Taiwan
[b] Institute of Electro-Optical Science and Technology, National Taiwan Normal University, Taipei 116, Taiwan
[c] Department of Electrical Engineering, Chunghua University, Hsinchu 300, Taiwan

ARTICLE INFO

Article history:
Received 6 November 2012
Accepted 19 December 2012
by X.C. Shen
Available online 3 January 2013

Keywords:
A. Superconductors
A. Photonic crystals
D. Wave properties

ABSTRACT

Effects of superconducting thin film on the defect mode in a dielectric photonic crystal heterostructure (PCH) are theoretically investigated. The considered structure is $(12)^N S(21)^N$, in which both layers 1 and 2 are dielectrics, layer S is a high-temperature superconducting layer, and N is the stack number. The defect mode is analyzed based on the transmission spectrum calculated by using the transfer matrix method. It is found that, in the normal incidence, the defect mode existing in the host PCH of $(12)^N(21)^N$ will be blue-shifted as the thickness of layer S increases. In addition, the defect mode is also blue-shifted for both TE and TM modes in the case of oblique incidence. The embedded superconducting thin film plays the role of tuning agent for the defect mode of PCH. As a result, the proposed structure can be designed as a tunable narrowband transmission filter which could be of technical use in the optoelectronic applications.

1. Introduction

One of the familiar applications in a one-dimensional photonic crystal (1D PC) is to engineer the photonic band gap (PBG) to design a multilayer Fabry-Perot resonator (FPR) also called the multilayer narrowband transmission filter. An FPR has two possible structures, i.e., $(HL)^N D(HL)^N$ and $(HL)^N D(LH)^N$, where H, L are the high- and low-index layers, D is the defect layer, and N is the number of periods of the host PC. A typical design of FPR is to use the quarter-wave stack, i.e., the optical thicknesses of H, L and D, $n_H d_H = n_L d_L = n_D d_D = \lambda_0/4$, where λ_0 is the so-called design wavelength usually assigned in the vicinity of center of PBG. In general, the presence of D can produce a transmission peak in the transmission spectrum. This peak is referred to as a photonic defect mode which is similar to the impurity state in the electronic band gap of a doped semiconductor. There have been many reports on the properties of photonic defect modes in 1D PCs [1–5].

From the application point of view, a tunable filter will be of technical use in photonics and optoelectronics. To arrive at the tunability in a multilayer transmission filter, the defect material plays the dominant role. For instance, using semiconductor as a defect material, tunable feature is achievable because the dielectric function is a function of the carrier concentration $\tilde{N}$ and the temperature T [4,6,7]. Taking the liquid crystal as a defect layer, the transmission peak can be controlled by the external electric field [8–10]. If the magnetic material is used for the defect layer, we can thus have a magnetically tunable filter [11–15].

In addition to the above-mentioned PCs, PCs containing superconductors have also attracted much attention recently [16–20]. Most works primarily focus on the properties of photonic band structures in the superconductor-dielectric photonic crystals (SDPCs). In [16], the use of SDPC can be enhanced the omnidirectional PBG, which can be employed to design a wide band mirror. In [17], temperature-dependent resonant transmission in a lossy SDPC is investigated. In [18], a design of terahertz multichannel filter can be achieved in a finite SDPC containing high-temperature superconductor. The thickness-dependent PBG structure is analyzed in [19]. And the PBG structure in a two-dimensional SDPC is calculated in [20]. There are few reports on the optical properties of a defective dielectric–dielectric PC that contains a superconducting material as a defect layer.

In this work, we consider a dielectric–dielectric photonic crystal heterostructure (PCH) containing a superconducting defect, i.e., $(12)^N S(21)^N$, in which both layers 1 and 2 are dielectrics, layer S is a high-temperature superconducting layer, and N is the stack number. We first find that there is a defect mode in a PCH of $(12)^N(21)^N$. When superconducting layer S is embedded in between and structure is $(12)^N S(21)^N$, this defect mode can be tuned by the presence of S. It will be shown that the position of defect mode is blue-shifted as the thickness of S increases. In addition, it is also blue-shifted as a function of the angle of

* Corresponding author. Tel.: +886 2 77346724; fax: +886 2 86631954.
E-mail addresses: jasperwu@ntnu.edu.tw, chienjangwu@gmail.com (C.-J. Wu).

0038-1098/$ - see front matter © 2013 Elsevier Ltd. All rights reserved.
http://dx.doi.org/10.1016/j.ssc.2012.12.022

incidence for both TE and TM waves. The analysis made is based on the transfer matrix method (TMM) [21]. Finally, our results will be compared with the recent reports, in which the complex defect layer is considered [22–24].

2. Basic equations

In the beginning, we first describe the refractive index of the superconductor layer. The electromagnetic response of the superconductor in our structure can be well described by the two-fluid model together with the London local electrodynamics [25]. Taking the convention of $\exp(j\omega t)$ for the temporal part, the response function can be represented by the complex conductivity,

$$\sigma(\omega,T)=\sigma_n+\sigma_s=\sigma_{dc}\left[\frac{1}{1+\omega^2\tau^2}x_n-j\left(\frac{\omega\tau}{1+\omega^2\tau^2}x_n+\frac{1}{\omega\tau}x_s\right)\right] \quad (1)$$

where $\sigma_{dc}=ne^2\tau/m$ is the normal-state static conductivity, $x_s=1-x_n=n_s(T)/n$ is the fraction of the super-electrons, where $n_s(T)$ is the temperature-dependent super-electron density and n is the total electron density. The expression for $n_s(T)/n$ is given by the Gorter-Casimir relation, namely

$$\frac{n_s}{n}=1-\left(\frac{T}{T_c}\right)^4 \quad (2)$$

where T_c is the critical temperature of the superconductor. In this work, we shall limit to the lossless superconductor. That is, the operating temperature is well below T_c. In this case, the loss term contributed by the normal electrons can be negligibly small and thus Eq. (1) reduces to

$$\sigma(\omega,T)=-j\frac{n_se^2}{m\omega}=-j\frac{1}{\omega\mu_0\lambda_L^2} \quad (3)$$

where the temperature-dependent London penetration depth is

$$\lambda_L\equiv\sqrt{\frac{m}{\mu_0n_s^2e^2}}=\frac{\lambda_0}{\sqrt{1-\left(\frac{T}{T_c}\right)^4}} \quad (4)$$

where λ_0 is the London penetration depth at $T=0$ K. With Eq. (3), the dielectric function of the superconductor is obtained to be

$$\varepsilon_s=1-j\frac{\sigma(\omega,T)}{\omega\varepsilon_0}=1-\frac{1}{\omega^2\mu_0\varepsilon_0\lambda_L^2} \quad (5)$$

The refractive index of the superconductor layer is thus given by

$$n_s=\sqrt{\varepsilon_s}=\sqrt{1-\frac{1}{\omega^2\mu_0\varepsilon_0\lambda_L^2}} \quad (6)$$

It can be seen that the refractive index of the superconductor is dependent on the frequency and the temperature as well.

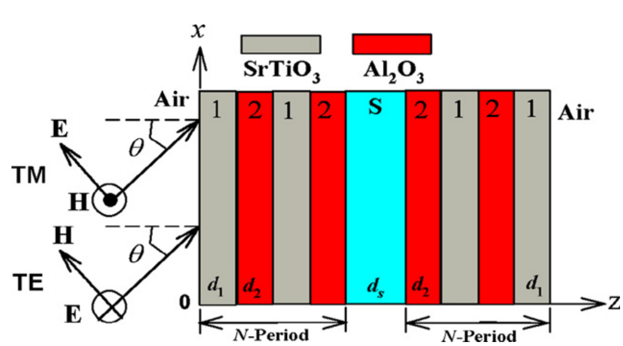

Fig. 1. The structural diagram of $(1/2)^N S(2/1)^N$, where the thicknesses of 1, 2, and S are denoted by d_1, d_2, and d_s, respectively, and the $D=d_1+d_2$ is the spatial periodicity.

Let us now consider the filter structure shown in Fig. 1, in which the superconducting layer S is embedded in the center of PCH. The refractive index of layer S is given in Eq. (6). The refractive indices of layers 1 and 2 are denoted by n_1 and n_2, respectively. The thicknesses are d_1, d_2, and d_s for the layers 1, 2 and S, respectively. The filtering properties will be analyzed through the transmittance spectrum calculated by the TMM [21]. According to TMM, the total system matrix is written by

$$M_{system}=\begin{pmatrix} m_{11} & m_{12}\\ m_{21} & m_{22}\end{pmatrix}=D_0^{-1}(M_1M_2)^N M_s(M_2M_1)^N D_0 \quad (7)$$

where the single-layer matrix is given by

$$M_i=D_iP_iD_i^{-1},\quad i=1,2 \quad (8)$$

Here, the propagation matrix in layer i is expressed as

$$P_i=\begin{pmatrix}\exp(jk_id_i) & 0\\ 0 & \exp(-jk_id_i)\end{pmatrix} \quad (9)$$

where $k_i=k_0n_i$, $i=1$, 2, and S, is the wave number in layer i, respectively, and $k_0=\omega/c$ is the free-space wave number, The dynamical matrix in medium i is written by

$$D_i=\begin{pmatrix}1 & 1\\ n_i\cos\theta_i & -n_i\cos\theta_i\end{pmatrix} \quad (10)$$

for the TE wave, and

$$D_i=\begin{pmatrix}\cos\theta_i & \cos\theta_i\\ n_i & -n_i\end{pmatrix} \quad (11)$$

for the TM wave, respectively. The transmittance is then given by

$$\Gamma=\left|\frac{1}{m_{11}}\right|^2 \quad (12)$$

3. Numerical results and discussion

In the following numerical calculations, the material parameters of superconducting layer S will be taken on the order of typical system of $YBa_2Cu_3O_{7-x}$ (YBCO), that is, $T_c=92$ K, $\lambda_0=200$ nm. The dielectric layer 1 is $SrTiO_3$ and layer 2 is Al_2O_3 because these two dielectric materials are widely used as the substrates for YBCO. The refractive indices for $SrTiO_3$ and Al_2O_3 are $n_1=2.437$ and $n_2=1.767$, respectively [22,23,26]. In the first panel of Fig. 2, we have plotted the transmittance for a finite bare PC of $(1/2)^{20}$. Here, we take $a=d_1+d_2=1$ μm, where $d_1=0.42a$ and $d_2=0.58a$ are chosen. It can be seen that there exist a PBG with the left band edge near $\omega a/2\pi c=0.22$ and the right band edge near $\omega a/2\pi c=0.27$. Next, when the PCH, $(12)^{10}(21)^{10}$, is formed, a resonant peak is found at $\omega_p a/2\pi c=0.244$, as shown in the second panel of Fig. 2. Now, with the insertion of superconducting layer S operating at $T=4.2$ K, the resonant peak in the second panel is shifted to the right, indicating a blue-shift effect. The dotted vertical line marks the position of peak in the absence of S. The blue-shift continues as the thickness of S increases. The dependence of peak $\omega_p a/2\pi c$ frequency on d_s is plotted in Fig. 3, in which a nearly linear dependence is seen.

The above-discussed results are analyzed in the simple normal incidence case. We now turn our attention to the oblique incidence, in which there are two possible polarizations of the incident wave, i.e., the TE and TM waves. In Fig. 4, we have plotted the TE-wave transmittance spectra for $d_s=20$ nm at distinct angles of incidence, $\theta=0°$, 15°, 30°, 45°, 60°, and 75°. It can be seen that the peak frequency is blue-shifted as the angle of incidence increases. The dependence of peak $\omega_p a/2\pi c$ frequency on θ is shown in Fig. 5. Some features are of note. First, the

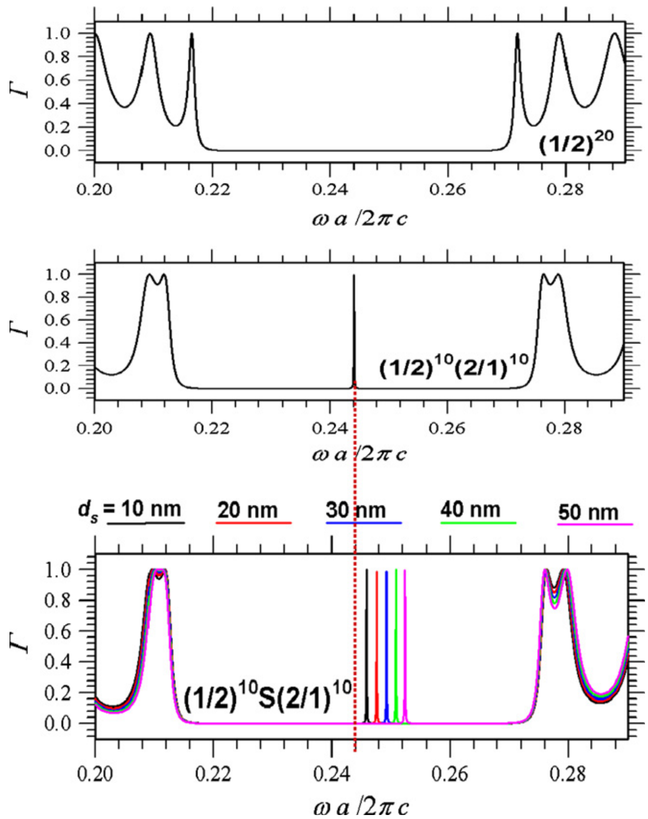

Fig. 2. The calculated transmittance spectra for $(1/2)^{20}$ (first panel), $(1/2)^{10}(2/1)^{10}$ (second panel), and $(1/2)^{10}S(2/1)^{10}$, with different thickness in S (third panel).

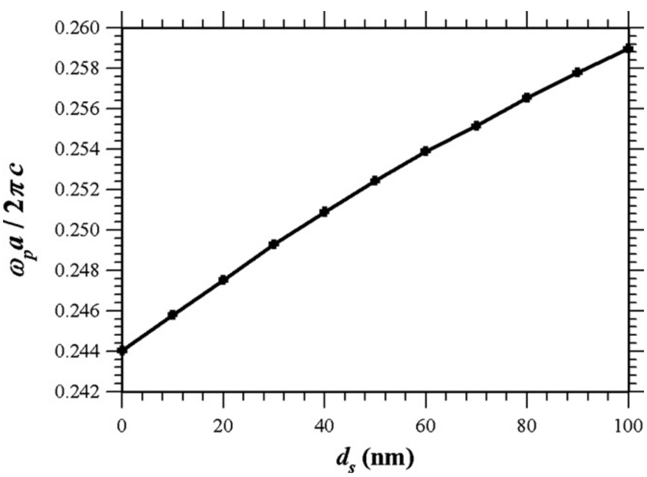

Fig. 3. The peak frequency ($\omega_p a/2\pi c$) as a function thickness of superconducting layer (d_s).

increasing trend is not linear-like as seen in Fig. 3. Second, in the TE wave, the entire transmittance spectrum has been shifted to the right as the angle increases. In addition, the width of PBG is also enlarged such that, at a large angle of 60^0, the transmission peak is moved outside the PBG of $\theta=0^\circ$. Finally, the range of variation in $\omega_p a/2\pi c$ in Fig. 5 is clearly larger than that in Fig. 3, indicating that the shifting effect is more pronounced due to the angle of incidence compared to the thickness of the superconducting film. The similar blue-shift is also seen for the TM wave, as illustrated in Fig. 6, in which the transmission peak moves to the right as θ increases. Conclusively, the transmission peak can be tuned by the superconducting film thickness and the angle of incidence for both TE and TM waves.

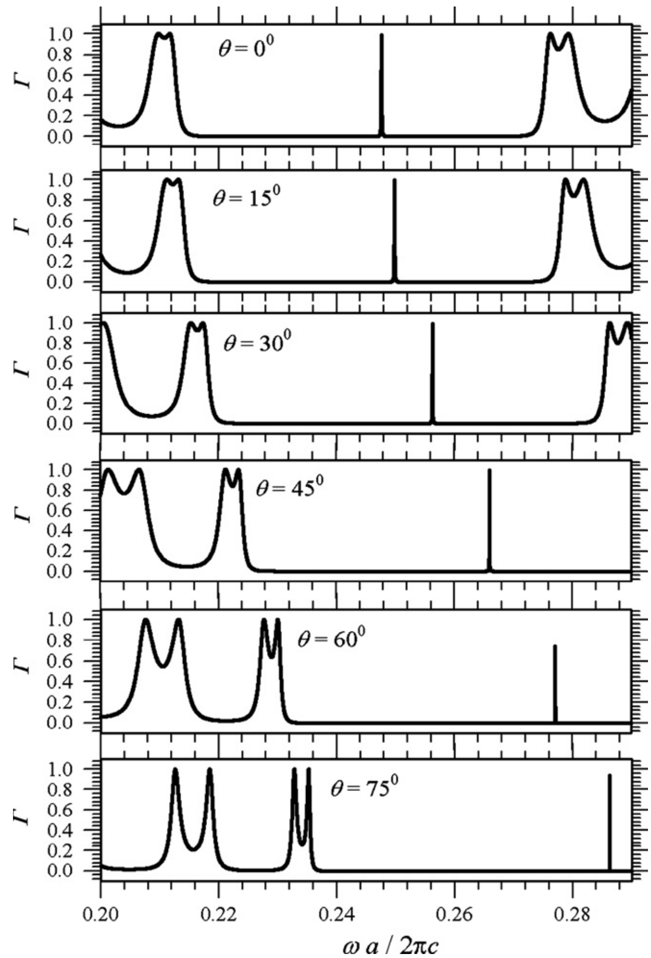

Fig. 4. Calculated TE-wave transmittance spectra at different angles of incidence, $\theta=0^\circ$, 15°, 30°, 45°, 60°, and 75°, respectively, with d_s=20 nm and T=4.2 K.

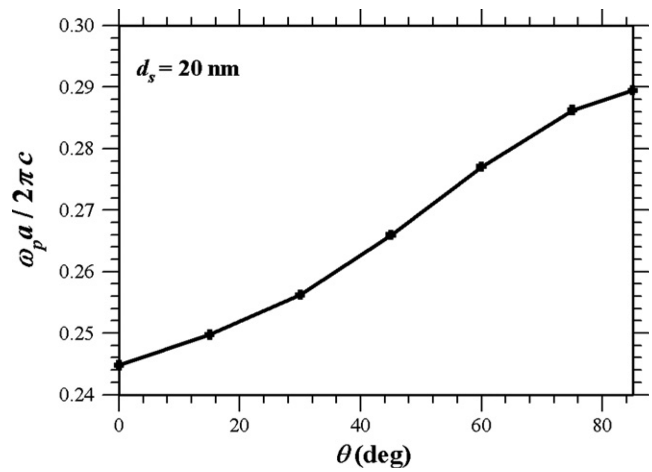

Fig. 5. The peak frequency versus the angle of incidence under the TE wave.

Before conclusion, let us make a comparison of the above results with previous reports [22,23]. In the normal incidence, the peak frequency shift as a function of superconducting film thickness is consistent with the Ref. [22]. In the oblique incidence, our results also agree with those in Ref. [23]. However, in Refs. [22] and [23], the authors consider a complex defect (with a superconducting film and a dielectric layer) in a PC. In this work,

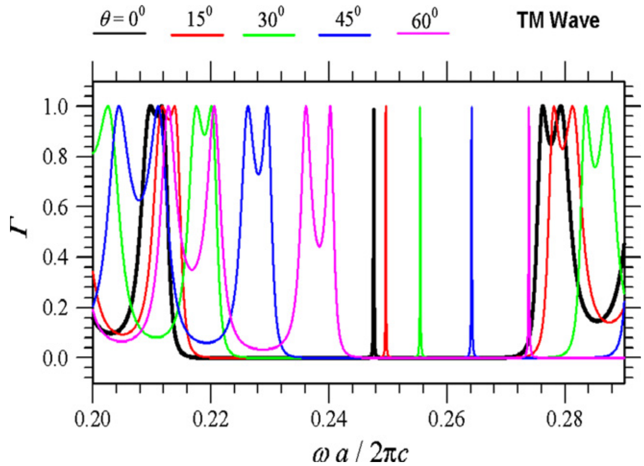

Fig. 6. Calculated TM-wave transmittance spectra at different angles of incidence, $\theta=0^\circ$, 15°, 30°, 45°, and 60°, respectively, with $d_s=20$ nm and $T=4.2$ K.

we have considered a single superconducting defect in a PCH. So, our structure is more simple and easy to fabricate experimentally.

4. Conclusion

By adding a superconducting thin film in the middle of dielectric PCH, the property of defect mode appearing in the PBG of the original PC has been analyzed in this work. We have illustrated the role played by this superconducting thin film. That is, superconducting thin film is not a source of the defect mode even it looks like defect in the structure. It works as a tunable agent for the defect mode, which is shown to be blue-shifted as the thickness of superconducting film increases. The defect mode can also move to the higher frequency when the angle of incidence increases for both TE and TM waves. Thus, the analysis presented here suggests an alternative that can be used to design a tunable narrowband transmission filter based on the use of a dielectric PCH containing a superconducting thin film.

Acknowledgment

C.-J. Wu acknowledges the financial support from the National Science Council of the Republic of China (Taiwan) under Contract No. NSC-100–2112-M-003–005-MY3. The authors are also greatly indebted to Prof. I. L. Lyubchanskii for his valuable suggestions and comments.

References

[1] S.J. Orfanidis, Electromagnetic Waves and Antennas, Rutger University, New Jersey, 2010. (Chapter 7).
[2] Y.-H. Chang, Y.-Y. Jhu, C.-J. Wu, Opt. Commun. 285 (2012) 1501.
[3] Y. Liu, Z. Lu, Prog. Electromagn. Res. 112 (2011) 257.
[4] H.-C. Hung, C.-J. Wu, S.-J. Chang, J. Appl. Phys. 110 (2011) 093110.
[5] C.-J. Wu, Z.-H. Wang, Prog. Electromagn. Res. 103 (2010) 169.
[6] P. Halevi, F. Ramos-Mendieta, Phys. Rev. Lett. 8 (2000) 1875.
[7] X. Dai, Y. Xiang, S. Wen, H. He, J. Appl. Phys. 109 (2011) 053104.
[8] P.K. Choudhury, W.K. Soon, Prog. Electromagn. Res. 104 (2010) 449.
[9] D. McPhail, M. Straub, M. Gu, Appl. Phys. Lett. 87 (2005) 091117.
[10] P. Halevi, J.A. Reyes-Avendano, J.A. Reyes-Cervantes, Phys. Rev. E 73 (2006) R040701.
[11] H. Tian, J. Zi, Opt. Commun. 252 (2005) 321.
[12] H.-C. Hung, C.-J. Wu, T.-J. Yang, S.-J. Chang, IEEE Photonic. J. 4 (2012) 903.
[13] C. Sabah, S. Uckun, Prog. Electromagn. Res. 91 (2009) 349.
[14] M. Inoue, R. Fujikawa, A. Baryshev, A. Khanikaev, P.B. Lim, H. Uchida, O. Aktsipetrov, A. Fedyanin, T. Murzina, A. Granovsky, J. Phys. D Appl. Phys. 39 (2006) R151.
[15] I.L. Lyubchanskii, N.N. Dadoenkova, M.I. Lyubchanskii, E.A. Shapovalov, Th. Rasing, J. Phys. D Appl. Phys. 36 (2003) R227.
[16] X. Dai, Y. Xiang, S. Wen, Prog. Electromagn. Res. 120 (2011) 17.
[17] C.H. Raymond Ooi, Q. Gong, J. Appl. Phys. 110 (2011) 063513.
[18] W.-H. Lin, C.-J. Wu, T.-J. Yang, S.-J. Chang, Opt. Exp. 18 (2010) 27155.
[19] C.-J. Wu, C.-L. Liu, W.-K. Kuo, J. Electromagn. Waves Appl. 23 (2009) 1113.
[20] O.L. Bermann, Y.E. Lozovik, S.L. Eiderman, R.D. Coalson, Phys. Rev. B 74 (2006) 092505.
[21] P. Yeh, Optical Waves in Layered Media, John Wiley & Sons, Singapore, 1991.
[22] I.L. Lyubchanskii, N.N. Dadoenkova, A.E. Zabolotin, Y.P. Lee, Th. Rasing, J. Optics: Pure and Appl. Optics 36 (2009) 114014.
[23] N.N. Dadoenkova, A.E. Zabolotin, I.L. Lyubchanskii, Y.P. Lee, Th. Rasing, J. Appl. Phys 108 (2010) 093117.
[24] J. Barvestani, Opt. Comm. 284 (2011) 231.
[25] T.V. Duzer, C.W. Turner, Principle of Superconductive Devices and Circuits, Prentice Hall, London, 1981.
[26] E.D. Palik, Handbook of Optical Constants of Solids, Academic, New York, 1991.